Towards understanding MgO/Fe interface formation: Adsorption of O and Mg atoms on an Fe(001) surface

Damian Wiśnios,[1,2] Adam Kiejna,[2,*] and Józef Korecki[1,3]

[1]*Faculty of Physics and Computer Science, AGH University of Science and Technology, al. Mickiewicza 30, 30-059 Kraków, Poland*

[2]*Institute of Experimental Physics, University of Wrocław, Plac M. Borna 9, 50-204 Wrocław, Poland*

[3]*Jerzy Haber Institute of Catalysis and Surface Chemistry, Polish Academy of Sciences, ul. Niezapominajek 8, 30-239 Kraków, Poland*

(Received 17 March 2017; revised manuscript received 16 July 2017; published 11 September 2017)

We report results of first-principles study of the adsorption of atomic oxygen and magnesium on the Fe(001) surface. Two adsorption scenarios were considered. In the first process, the Mg atoms were adsorbed on the Fe(001) surface with preadsorbed O atoms, whereas in the second scenario metallic Mg preadsorbed on the Fe(001) surface was exposed to oxygen. For both O and Mg atoms, fourfold hollow sites were found as the energetically most favorable adsorption sites on the clean Fe(001) surface. The result of both adsorption scenarios was the formation of a MgO adlayer on the Fe(001) surface with a sharp MgO/Fe interface. In particular, the deposition of Mg atoms on O/Fe(001) showed that magnesium can pull out O adatoms from the Fe surface. Structural, electronic, and magnetic properties were analyzed as a function of O and Mg coverages. The calculated electronic structure and magnetic moments showed that the full MgO monolayer affects the properties of the Fe surface much weaker than an incomplete MgO adsorbate layer.

DOI: 10.1103/PhysRevB.96.115418

I. INTRODUCTION

Metal-oxide heterostructures [1] have been widely investigated for many years. In particular, the combination of these two different materials in Fe/MgO systems is the origin of many interesting properties such as enhanced magnetic moments [2], interlayer exchange coupling [3,4], tunneling magnetoresistance [5,6], or perpendicular magnetic anisotropy [7,8]. These phenomena largely depend on the interface structure between metal and oxide; hence, a deep understanding of the metal-oxide interface is a key issue for technological applications, such as catalysis or spintronics.

The significant role of layered structures consisting of Fe and MgO, as cited above, is related to their structural simplicity and the small lattice mismatch between the surface MgO(001) and Fe(001) unit cells (≈4%). This results in a good epitaxial growth of Fe on MgO and MgO on Fe [9–12]. Understanding the magnetic and transport properties of the MgO/Fe(001) and Fe/MgO(001) systems is impossible without a detailed analysis of the structure of the MgO/Fe interface. During the formation of the MgO/Fe(001) system, both the sharp, nonoxidized MgO/Fe [13,14] and oxidized MgO/FeO/Fe interface [15,16] should be taken into account. The presence of Fe-O bonds in the interface can significantly affect the spin polarization of the Fe atoms [17]. An observed interface type crucially depends on the preparation conditions, in particular, the amount of oxygen present (O-deficient or O-rich conditions) plays a crucial role [18].

Theoretical papers referred to the MgO/Fe interface consider the equilibrium and relaxed structure. The authors assume commonly predetermined adsorption sites above the iron substrate. Some of them noticed [15,16] that methods and conditions of growth can play a crucial role in the structure of the interface between MgO and Fe. Interactions between adsorbed atoms and the substrate may cause significant changes in the adsorption geometry. Therefore, the detailed investigation of the first step of growth is essential to understand the processes taking place during the formation of the MgO/Fe interfaces and the role of its structure on properties of the multilayered systems.

The formation of the MgO(001)/Fe(001) interface can be considered to be composed of single adsorption events both of MgO molecules and of atomic oxygen and magnesium on the Fe surface. The latter process should depend on the sequence of adsorption events: either adsorption of the O atoms on the clean Fe(001) surface is followed by adsorption of the Mg atoms on the O/Fe(001) surface, or the adsorption order is reversed, i.e., first, the Mg atoms are adsorbed, and then the Mg-decorated Fe(001) surface is exposed to oxygen. Both processes can occur as transient states in different experimental realizations of epitaxial growth of MgO(001) on Fe(001). MgO can be deposited from bulk using a thermal source, and in this case, in the molecular beam, both molecular and atomic species are present [19,20]. To ensure proper MgO stoichiometry, the above process can be conducted with an oxygen background pressure. Alternatively, MgO layers can be grown by reactive deposition of metallic Mg in an oxygen atmosphere [21] or by exposure of metallic Mg (mono)layers on Fe to oxygen [22]. Finally, these two adsorption sequences, which are discussed in this paper, can be directly realized if MgO is grown on Fe(001)-$p(1 \times 1)$O [14] or on Fe(001) precovered with Mg [21]. Thus, the adsorption of oxygen and magnesium on Fe(001) is a starting point of our study.

The oxidation of the Fe(001) surface has been investigated for more than 40 years. Early experimental low-energy electron diffraction, Auger-electron spectra, and electron-energy-loss spectroscopy (LEED, AES, and EELS) studies [23–25] showed that oxygen prefers chemisorption at the fourfold hollow sites on the Fe(001) surface, which results in 7.5% expansion of the first Fe-Fe interlayer spacing with respect to the bulk value. The experimental findings regarding the structure and the preferable adsorption sites were confirmed by theory [26–28]. Chubb and Pickett [27] reported that the

*adam.kiejna@uwr.edu.pl

first Fe-Fe interlayer spacing is relaxed by 23% and they noticed that an Fe surface with adsorbed O atoms is similar to a rock-salt FeO monolayer which is weakly bound to the substrate. A more detailed analysis of the O/Fe(001) system presented by Bonell *et al.* [29] showed that below 1 monolayer (ML) coverage of oxygen, a disordered surface phase is formed, with oxygen located mainly at the fourfold hollow sites. Higher coverage alters the adsorption kinetics to the condensed phase, resulting in the formation of FeO islands and the $p(1 \times 1)$-O phase on the rest of the surface. Investigation of the $p(1 \times 1)$-O/Fe(001) structure was carried out by Parihar *et al.* [30]. The authors confirmed the location of oxygen at the fourfold hollow site at a distance of 0.48 Å from the first Fe layer, and they reported a large 16% increase of the first Fe-Fe interlayer spacing relative to the bulk spacing.

The adsorption of oxygen causes modifications to the magnetic properties. An enhancement of the magnetic moments on the Fe atoms in the first and second layers, which is a result of the increase in separation between the uppermost Fe layers, was reported. First-principles calculations [31] showed that oxygen adsorption contributes to an increase in the magnetic moment on surface Fe atoms to $3.23\mu_B$ and stabilization of the ferromagnetism of the Fe(001) surface.

Much less effort has been devoted to the adsorption of Mg on Fe(001). This process has been experimentally studied as an initial stage of MgO formation. Dugerjav *et al.* [22] deposited Mg on the Fe(001) surface at room temperature, and then the sample was annealed at 300 °C under O_2 exposure. The procedure yielded high-quality MgO film on Fe(001), with Mg at the hollow sites and O on top of the Fe atoms. The adsorption of magnesium on the FeO/Fe(001) surface was studied experimentally by Oh *et al.* [16]. They observed that part of the oxygen from the FeO layer is transferred to Mg to form the MgO layer.

In our previous work, we considered the adsorption of MgO molecules on the Fe(001) surface [20]. A preference for the adsorption of MgO molecules aligned parallel to the surface was found, with the Mg atom at the fourfold hollow site and O atom on top of the Fe atom. As a result, a sharp, nonoxidized MgO/Fe interface between the MgO adlayer and Fe surface was formed. The possibility for the perpendicular adsorption of molecules with O atoms facing the surface at the hollow sites was also observed. For such a configuration, O atoms approached the surface and the onset of Fe-O layer formation was observed, which could result in the oxidized MgO/FeO/Fe interface.

Motivated by the diverse interface structures of the MgO/Fe interface, in this paper, we extend our first-principles calculation to the adsorption of single O and Mg atoms on the Fe(001) surface within two scenarios. In the first scenario, O atoms are adsorbed on the clean Fe(001) surface, followed by the adsorption of Mg atoms. In the second scenario, magnesium is adsorbed on the Fe(001) surface; subsequently, the Mg/Fe(001) structure is oxidized.

II. CALCULATION METHOD

The calculations were performed using the Vienna *ab initio* simulation package (VASP) and were based on the density functional theory (DFT) [32,33]. The exchange-correlation energy was treated using the Perdew-Burke-Ernzerhof (PBE) version [34] of the spin-polarized generalized gradient approximation (GGA) [35,36]. The electron-ion interactions were described by projector augmented-wave (PAW) potentials [37]. A cutoff energy of 400 eV was applied for the plane-wave-basis set. Brillouin zone integrations were performed using a special k-points mesh generated via the Monkhorst-Pack method [38]. The number of k points corresponded to a $6 \times 6 \times 1$ mesh for the 2×2 and a $4 \times 4 \times 1$ mesh for the 3×3 Fe(001) surface unit cell. The partial occupancies were determined via the first-order Methfessel-Paxton method [39], with a Fermi smearing of 0.2 eV. In the calculations, a lattice constant of 2.832 Å was applied, which was optimized in our previous work [20]. The Fe(001) surface was modeled using a slab of 9 Fe layers with the 3×3 (or 2×2) surface periodicity, separated from its periodic images by a vacuum region of 17 Å. The positions of atoms in three bottom layers were frozen. The positions of the remaining atoms of the slab were relaxed until the forces exerted on each atom were less than 0.01 eV/Å. Oxygen and magnesium atoms were adsorbed on one side of the slab. Dipole correction was applied [40], which is essential for calculating the correct work functions.

The adsorption energy of O and Mg atoms adsorbed on a clean Fe(001) surface was calculated from the total energy difference:

$$E_{\mathrm{ad}} = -\frac{1}{N}(E_{X/\mathrm{Fe}(001)} - E_{\mathrm{Fe}(001)} - NE_X), \qquad (1)$$

where $E_{X/\mathrm{Fe}(001)}$ and $E_{\mathrm{Fe}(001)}$ represent the total energy of the slab with adsorbed X (O or Mg) atoms and the total energy of the clean slab, respectively, N is the number of the adsorbed atoms, and E_X is the half-energy of the isolated O_2 molecule or the energy of the free Mg atom. The Bader charges [41] on atoms were calculated using the program developed by Henkelman *et al.* [42].

III. RESULTS

The properties of the clean Fe(001) surface were determined in our previous work [20] to be in good agreement with those reported by other authors [43–45]. In the adsorption studies, in the first stage, O (Mg) atoms were adsorbed on the Fe(001) surface, with the coverage from a single atom in a 3×3 or 2×2 surface unit cell to 1 ML. Next, for the 1 ML O or Mg coverage, Mg (O) atoms were adsorbed from $\frac{1}{9}$ ($\frac{1}{4}$) to 1 ML coverage. The O (Mg) atoms were initially adsorbed at three adsorption sites: the fourfold hollow (fhl) between four surface Fe atoms, on-top (ot) of the surface Fe atom, and the bridge (bri) site between two surface Fe atoms.

A. Energetics and geometry

1. Adsorption of Mg on O/Fe(001) surface

O adsorption on clean Fe(001) surface. The calculations showed that oxygen adsorption at the hollow site is more preferred than at other sites. The adsorption energy of a single O atom at the fhl site, i.e., 3.38 eV, is 0.65 and 1.44 eV higher than at the bri and ot sites, respectively. These results agree well with previous studies of oxygen adsorption on the Fe(001) surface [26–28,30]. Correspondingly, for oxygen adsorbed at

TABLE I. O adsorption on clean Fe(001) surface. Adsorption energy E_{ad}, work function Φ, height of O atoms h_O, and relaxations Δ_{ij} (as a percentage of bulk interplanar spacing) of the three topmost interlayer Fe distances as functions of O coverage Θ_O.

Θ_O	E_{ad}	Φ	h_O	Relaxation (%)		
(ML)	(eV/atom)	(eV)	(Å)	Δ_{12}	Δ_{23}	Δ_{34}
0		3.86		−2.1	3.3	0.4
1/9	3.38	3.97	0.64	−0.3	3.0	0.8
3/9	3.36	4.07	0.59	4.1	2.2	1.0
5/9	3.28	4.21	0.54	7.3	1.4	0.8
7/9	3.12	4.37	0.50	10.7	1.1	0.7
1	2.94	4.44	0.45	15.7	1.1	0.7

TABLE II. Mg adsorption on O/Fe(001) surface. Heights of the O (h_O) and Mg (h_{Mg}) atoms and relaxations Δ_{ij} of the three topmost interlayer Fe distances as functions of Mg coverage Θ_{Mg}.

Θ_{Mg} (ML)	h_O (Å)	h_{Mg} (Å)	Relaxation (%)		
			Δ_{12}	Δ_{23}	Δ_{34}
0	0.45		15.7	1.1	0.7
1/9	0.54	2.34	14.5	0.9	0.7
3/9	1.29	2.35	12.4	0.1	0.8
5/9	1.76	2.49	7.1	0.6	0.9
7/9	2.20	2.37	3.0	1.4	0.5
1	2.25	2.14	−1.8	2.8	1.2

the most preferred position, coverage from $\frac{1}{9}$ ML (one O atom in a 3×3 surface unit cell) to 1 ML was calculated. The results, summarized in Table I, show that both the adsorption energy and the height of the O atoms above the surface (the bonding distance h_O) decrease with oxygen coverage (Θ_O). The O atoms of a complete monolayer are adsorbed 0.44 eV weaker than a single adatom. h_O shrinks from 0.64 Å ($\frac{1}{9}$ ML) to 0.45 Å (1 ML). Oxygen adsorption greatly increases surface relaxation, $\Delta_{ij} = (d_{ij} - d)/d$, of the distance between subsequent, i.e., i and $j = i + 1$, surface Fe layers, where d is the bulk interplanar spacing. Upon O adsorption, the calculated relaxation Δ_{12} changes from small, negative to large, positive values (Table I). For $\Theta_O = 1$, the first Fe-Fe interlayer spacing is expanded by 15.7% to 1.64 Å, compared with bulk Fe. This confirms the results of previous theoretical works [28,46].

Mg adsorption on O/Fe(001) surface. In this scenario, the oxygen precovered Fe(001) surface was the substrate for the adsorption of Mg atoms. For each stage of Mg coverage (Θ_{Mg}), a subsequent Mg atom was adsorbed at different available positions. The configuration with the lowest total energy was then used in the subsequent step of the Mg adsorption. Different stages of the Mg adsorption are illustrated in Fig. 1. It can be seen that adsorption of the Mg atoms caused significant displacements of the O atoms on the surface. As a result of the strong interaction between adsorbed Mg atoms and O atoms on the surface, oxygen tended to move from its most favorable fhl site to the bri or ot site. Then, the fhl site released by the O atom could be occupied by a Mg atom. Eventually, all O atoms shifted to positions on top of the Fe atoms, with all adsorbed Mg atoms occupying the hollow sites. In the Θ_{Mg} range from $\frac{3}{9}$ to $\frac{6}{9}$, one can notice a disordered Mg-O phase, where both O and Mg atoms occupy different adsorption sites. For higher Mg coverage, the adsorbate begins to form the MgO monolayer, with oxygen on top of Fe atoms and magnesium at the hollow sites. The final configuration is the MgO/Fe(001) system with a sharp interface. This result, albeit consistent with other theoretical and experimental studies [12,47] regarding MgO on the Fe(001) surface, is significant in that the magnesium atoms on the oxygen-saturated, i.e., FeO-like, Fe(001) surface cause reduction of the surface iron atoms.

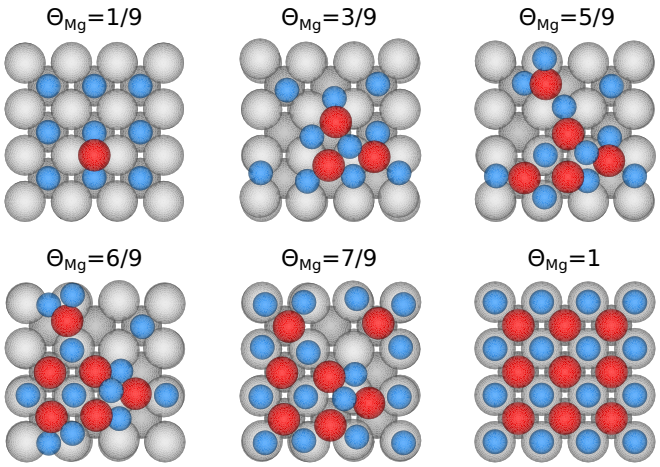

FIG. 1. Top view of the subsequent stages of the Mg adsorption on the O/Fe(001) surface. Red, blue, and gray balls represent Mg, O, and Fe atoms, respectively.

The interaction between O and Mg on the Fe(001) surface contributes to the systematic increase of the height of the O atoms above the surface. This distance rises from 0.45 to 2.25 Å for $\Theta_{Mg} = 1$, which is consistent with the MgO/Fe(001) structure [47]. After completion of the MgO monolayer, the Mg atoms are situated 0.11 Å lower than the O atoms, which results from the 4% lattice misfit between the MgO(001) and Fe(001) surfaces. The adsorption of Mg gradually restores the interlayer distances in the Fe substrate (Table II). This effect is especially seen in the relaxation of the first Fe-Fe distance Δ_{12}. After large expansion during the adsorption of O atoms, the first Fe-Fe interlayer distance contracts to 1.39 Å for 1 ML of Mg, which is close to the bulk interplanar spacing of 1.416 Å.

2. *Adsorption of O atoms on Mg/Fe(001) surface*

Mg adsorption on clean Fe(001) surface. For the adsorption of Mg atoms on the clean Fe(001) surface, the fhl sites are energetically most preferable. The adsorption of a single Mg atom on the Fe(001) surface at the fhl site ($E_{ad} =$ 1.50 eV) is 0.33 and 0.86 eV stronger than at the bri and ot sites, respectively. Therefore, the subsequent stages of the adsorption were calculated only for Mg at the fhl site.

In contrast to O adsorption, the binding energy of Mg increases with coverage, reaching nearly 2 eV/atom for the 1 ML Mg coverage (Table III). However, this is approximately 1 eV less than that for the O atoms adsorbed at the same

TABLE III. Mg adsorption on clean Fe(001) surface. Adsorption energy E_{ad}, work function Φ, height of Mg atoms h_{Mg}, and relaxations Δ_{ij} of the three topmost interlayer Fe distances as functions of Mg coverage Θ_{Mg}.

Θ_{Mg}	E_{ad}	Φ	h_{Mg}	Relaxation (%)		
(ML)	(eV/atom)	(eV)	(Å)	Δ_{12}	Δ_{23}	Δ_{34}
0		3.86		−2.1	3.3	0.4
1/4	1.50	3.38	1.73	−1.6	2.9	0.4
2/4	1.81	3.47	1.68	−0.7	1.8	0.2
3/4	1.94	3.35	1.77	0.4	1.7	0.4
1	1.98	3.46	1.77	−5.6	1.6	−0.2

TABLE IV. O adsorption on Mg/Fe(001) surface. Heights of the O (h_O) and Mg (h_{Mg}) atoms, and relaxations Δ_{ij} of the three topmost interlayer Fe distances as functions of O coverage Θ_O.

			Relaxation (%)		
Θ_O (ML)	h_{Mg} (Å)	h_O (Å)	Δ_{12}	Δ_{23}	Δ_{34}
0	1.77		−5.6	1.6	−0.2
1/4	1.89	2.39	−2.0	1.8	0.8
2/4	1.99	2.27	−1.3	2.1	1.2
3/4	2.10	2.31	−1.8	2.2	0.7
1	2.14	2.25	−1.9	2.8	1.1

adsorption site. Simultaneously, the Mg atoms lie much higher above the surface, at distances of 1.68–1.77 Å which only weakly depends on the coverage. These results indicate that Mg is not as bound to the Fe surface as oxygen. In contrast to the O adsorption, Mg adsorption induces contraction of the interplanar distance of the topmost Fe layers. For 1 ML coverage, the first Fe-Fe interlayer spacing is 5.6% smaller than that in the bulk Fe. Such contraction of the spacing can result from a smaller atomic volume in the bcc iron crystal in comparison with hcp magnesium. Mg atoms, which have too little available in-plane space on the Fe(001) surface, exert normal pressure on the substrate. In consequence, the iron surface is compressed.

O adsorption on Mg/Fe(001) surface. The adsorption geometries of oxygen on the Mg precovered Fe(001) surface are shown in Fig. 2. The adsorption of O atoms does not cause significant changes on the surface, even though the oxygen is adsorbed at the less preferred adsorption sites (on top of Fe atoms). This adsorption sequence leads to the same structure as for the adsorption of MgO molecules on the Fe(001) surface, which was studied in our previous work [20]. Additionally, the adsorption energy per MgO formula unit for a complete MgO monolayer (6.81 eV) agrees very well with the adsorption energy reported for the MgO molecule [20]. It also supports a previous experimental work [22], where post-oxidation of a Mg monolayer resulted in a MgO monolayer with high crystalline quality on the Fe(001) surface.

The adsorption of O atoms affects the heights of the adsorbate, as shown in Table IV. The adsorption of subsequent O atoms causes a gradual increase in the distance between Mg and the surface. In the whole range of O coverage, the O atoms are farther from the surface than the Mg atoms, which rumples the MgO adlayer. The largest rumpling is for the fractional coverages of oxygen adsorbed at the less preferable ot sites, but it decreases with coverage and, for the complete MgO monolayer, is as small as 0.11 Å, in agreement with previous studies of the MgO/Fe(001) system [47]. The influence of the adsorbate on the substrate relaxation (Table IV) is considerably smaller than during the reverse sequence of adsorption. Upon Mg adsorption, the first Fe-Fe distance is slightly reduced, but after adsorption of oxygen, is almost recovered to the value corresponding to the clean Fe(001) surface.

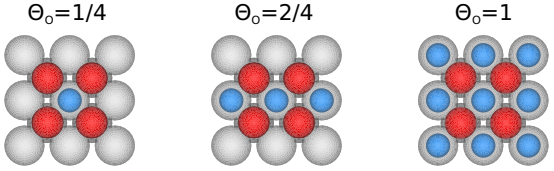

FIG. 2. Top view of the considered configuration of the O adsorption on the Mg/Fe(001) system for three different O coverages.

B. Work function and charge transfer

To better understand the rearrangement of the electron charge density in the Mg-O/Fe(001) systems, which determines adsorbate binding, we analyzed the electron work function, electron charge density changes induced by adsorbates, and Bader charges on the surface atoms.

Work function. The work function was calculated as the difference between the electrostatic potential energy in the vacuum region and the Fermi energy of the slab. Changes of the work function as a function of O and Mg coverage during the two scenarios of adsorption considered are presented in Fig. 3. Upon oxygen adsorption on the clean Fe(001) surface, the work function increases with oxygen coverage. For a complete oxygen monolayer, the work function of O/Fe(001) achieves 4.44 eV. Subsequent adsorption of a single Mg atom on an O-covered Fe(001) surface causes the work function to decrease to approximately 3.9 eV, which is close to the

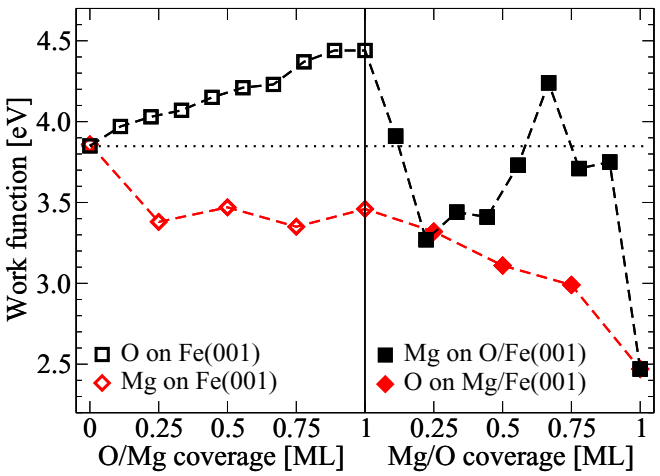

FIG. 3. Work function as a function of O and Mg coverage for two different adsorption scenarios. Dotted line indicates work function of the clean Fe(001) surface.

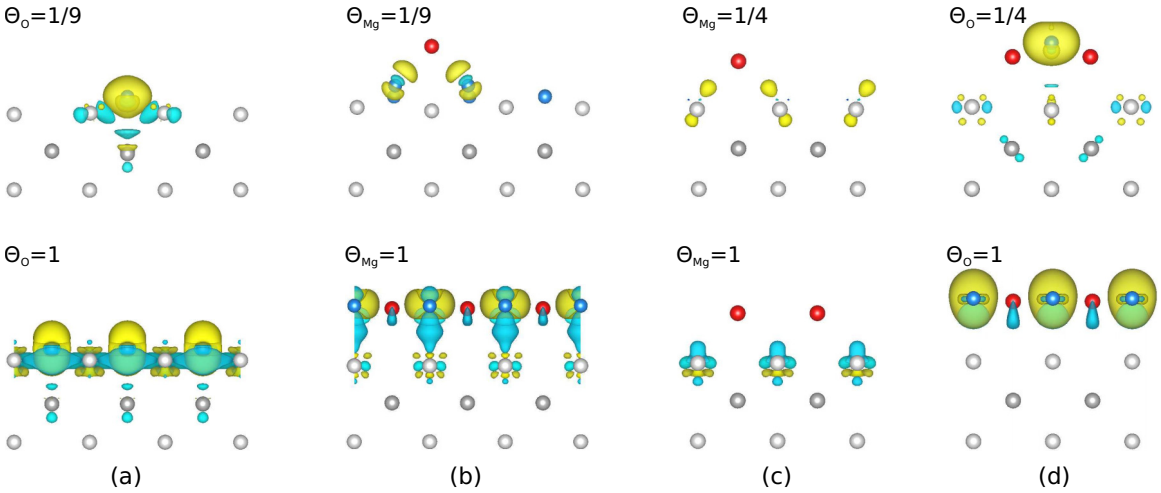

FIG. 4. Side view of isosurfaces of the valence charge density difference $\Delta\rho(\mathbf{r})$ for different adsorption scenarios: (a) O on Fe(001), (b) Mg on O/Fe(001), (c) Mg on Fe(001), and (d) O on Mg/Fe(001). Electron charge accumulation (depletion) is drawn in yellow (blue). Isosurface level is 0.007 e/a_0^3 (a_0 is the Bohr radius). Red, blue, and gray balls represent Mg, O, and Fe atoms, respectively.

value for the clean Fe(001) surface. By adding another Mg atom, the work function further diminishes to ≈3.3 eV. This work function reduction at the lowest Mg coverages is due to an increased surface roughness [48], which is largest for a single Mg adatom. Between $\Theta_{Mg} = \frac{2}{9}$ and $\frac{7}{9}$, the work function oscillates, which is due to the disordered Mg-O phase above the surface. With increased Mg coverage, the adsorbate layer becomes more ordered and both the surface structure and electron density become smoother, which, for $\Theta_{Mg} = \frac{6}{9}$, leads to the work function increasing to approximately 4.2 eV (Fig. 3). This smoothing effect competes with the effect of additional electrons provided by the Mg atoms, which saturate very electronegative oxygen ions. At still higher Θ_{Mg}, the latter effect starts to dominate and leads to the reduction of the work function to 2.47 eV for the full MgO monolayer. This agrees with our (2.45 eV) [20] and other [45] previous theoretical work regarding the MgO/Fe(001) structure.

In the second adsorption scenario, the work function decreases, showing weak oscillations, with both Mg and O coverage (Fig. 3). Adsorption of a single Mg atom on the clean Fe(001) surface reduces the work function by approximately 0.5 eV. Then, it remains almost constant up to the formation of a complete Mg monolayer, where it attains a slightly lower value than that of the clean Mg(0001) surface (3.76 eV) [49]. Upon the adsorption of oxygen on Mg/Fe(001), the work function further decreases. This contrasts with the adsorption of O atoms on the clean Fe(001) surface, where the work function increases with oxygen coverage. The final value of the work function after O adsorption on Mg/Fe(001) is the same as in the case of Mg adsorption on the O/Fe(001) surface (Fig. 3).

Electron charge density distribution. The above work function changes result from the adsorbate-induced electron charge density redistribution. In Fig. 4, we plot isosurfaces of the electron charge density difference $\Delta\rho(\mathbf{r})$, which is defined as

$$\Delta\rho(\mathbf{r}) = \rho^{\mathrm{ads/sub}}(\mathbf{r}) - \rho^{\mathrm{sub}}(\mathbf{r}) - \rho^{\mathrm{ads}}(\mathbf{r}), \qquad (2)$$

where $\rho^{\mathrm{ads/sub}}$ is the electron density of the adsorbate/substrate system [O/Fe(001), MgO/Fe(001), or Mg/Fe(001)], ρ^{sub} is the electron density of the substrate system [Fe(001), O/Fe(001), or Mg/Fe(001)], and ρ^{ads} is the electron density of the isolated O and Mg adsorbate. ρ^{sub} and ρ^{ads} are calculated for the configuration corresponding to that of the relaxed adsorbate/substrate system.

O adsorption on the Fe(001) surface induces pronounced changes in $\Delta\rho(\mathbf{r})$. In Fig. 4(a), a significant charge transfer from the Fe atoms of the first and second Fe layer to the adjacent O atoms and formation of the strong bonding between the neighbouring O and Fe atoms can be seen. A depletion of the electron charge around the Fe atoms in the first layer and its accumulation around the O atoms contributes to an increase in the work function. Subsequent adsorption of the Mg atoms on the O-precovered surface entails further changes in the electron charge distribution [Fig. 4(b)]. The charge provided by the Mg atoms is transferred to the oxygen and Fe atoms and results in a decrease of the work function. Reduction of the charge in the region between O and the surface Fe atoms and charge accumulation around the O atoms, which are pushed away from the Fe surface [cf. $\Theta_{Mg} = 1$ in Fig. 4(b)], suggest weakening of the O-Fe bonding and the formation of stronger Mg-O bonds.

The adsorption of a Mg atom on the clean Fe(001) surface does not cause significant changes in the electron charge density distribution around surface atoms [Fig. 4(c)] but induces a considerable charge transfer between the Fe surface and the Mg adatoms, as is manifested by large changes in the Bader charges, which is discussed in the following paragraph. For $\Theta_{Mg} = 1$, a slight reduction of the charge between the Mg adlayer and surface Fe atoms can be seen, as well as some charge accumulation between the first and second Fe layer. This electron charge transfer from Mg to the Fe surface atoms leads to a work function decrease. Subsequent adsorption of the O atoms on the Mg/Fe(001) substrate induces further changes in $\Delta\rho(\mathbf{r})$ [Fig. 4(d)]. The electron charge accumulates around the O atoms and reduces between the MgO adlayer and Fe substrate. The O atoms take some electron charge from the Fe and Mg atoms, which leads to a bond weakening between the adsorbate and the surface. These effects contribute to a

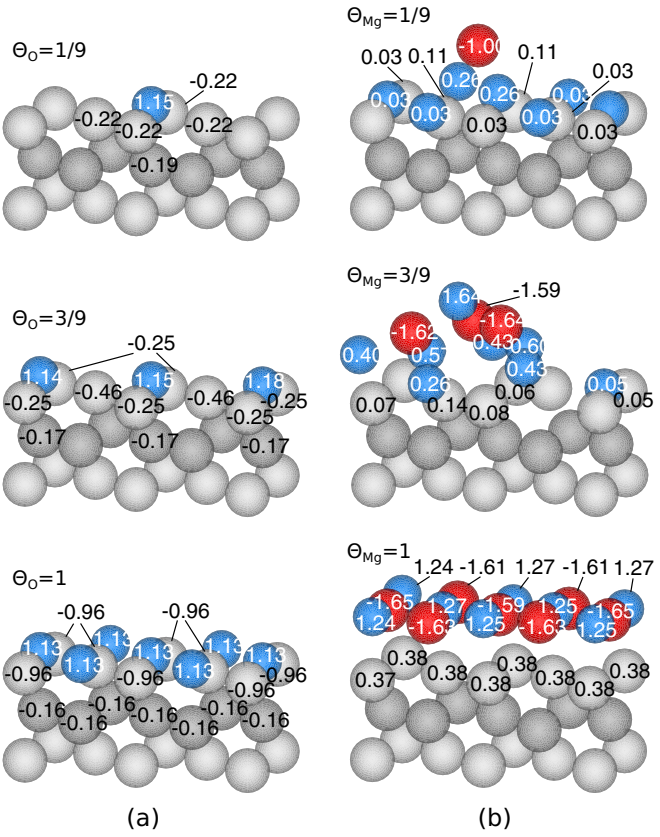

FIG. 5. Bader charge difference ΔQ on surface atoms, resulting from (a) O adsorption on the Fe(001) surface and (b) Mg adsorption in the O/Fe(001) system. The charges on Fe atoms below $0.03e$ are neglected. For the full MgO monolayer, the absolute values of the Bader charge on the surface Fe atoms, O and Mg atoms are $7.99e$, $7.57e$, and $0.36e$, respectively.

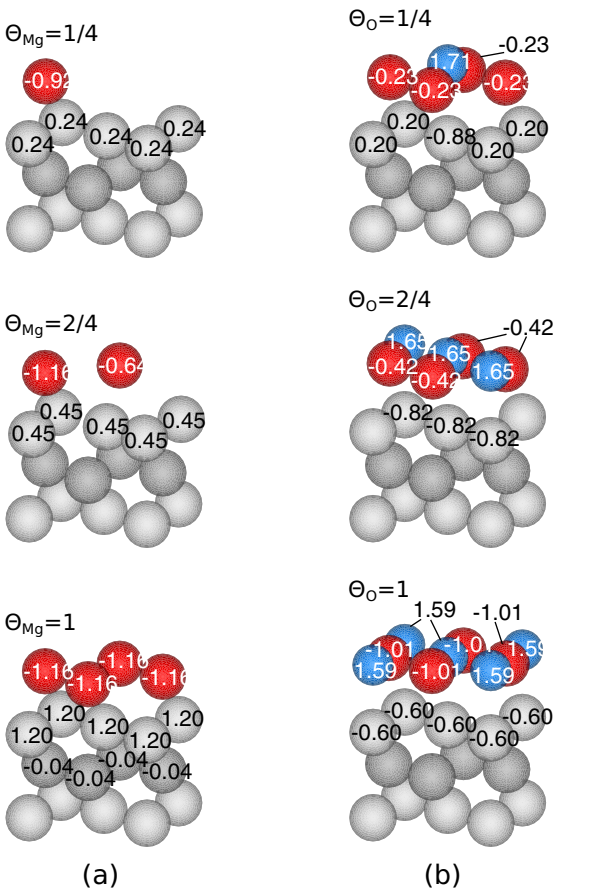

FIG. 6. Same as in Fig. 5 but for ΔQ resulting from (a) Mg adsorption on the Fe(001) surface, and (b) O adsorption in the Mg/Fe(001) system. For the full MgO monolayer, the absolute values of the Bader charge on the surface Fe atoms, O and Mg atoms are $7.98e$, $7.58e$, and $0.36e$, respectively.

decrease of the electrostatic potential in the vacuum region, which, with the simultaneous increase of the Fermi energy, leads to a lowering of the work function.

Bader charges. To quantify the electron charge transfer due to the adsorption, we have performed Bader charge analysis which allows us to attribute the electronic charge to every atom, and we have calculated the following charge difference:

$$\Delta Q = Q^{\mathrm{ads/sub}} - Q^{\mathrm{sub}} - Q^{\mathrm{ads}}. \tag{3}$$

Here, $Q^{\mathrm{ads/sub}}$ is the Bader charge on atoms of the adsorbate/substrate system [O/Fe(001), MgO/Fe(001), or Mg/Fe(001)], Q^{sub} is the charge on atoms of the substrate system [Fe(001), O/Fe(001), or Mg/Fe(001)], and Q^{ads} is the charge of the isolated O or Mg adsorbate. Q^{sub} and Q^{ads} are calculated in the configuration corresponding to that of the relaxed adsorbate/substrate system. The calculated differences ΔQ for the Mg/O/Fe(001) and O/Mg/Fe(001) adsorption systems are presented in Figs. 5 and 6, respectively. Upon O adsorption, electronegative O atoms draw electrons from adjacent Fe atoms of the first and second Fe layers [Fig. 5(a)]. Depending on the O coverage and adlayer configuration, each of the O atoms gains $1.13e$–$1.18e$. For higher O coverage, the Fe atoms of the two topmost layers are positively charged. Upon Mg adsorption on the O-precovered Fe(001) surface [Fig. 5(b)], the O atoms mainly draw electrons from the adsorbate and not from the Fe surface atoms. Small differences in ΔQ on Mg and O atoms of the same layer, for $\Theta_{\mathrm{Mg}} = 1$, are probably due to the small rumpling of the MgO layer.

The adsorption of Mg atoms on clean Fe(001) induces a considerable electron charge transfer from the Mg adatoms to the Fe surface atoms [Fig. 6(a)]. All Mg adatoms are positively charged, i.e., they are cationic. Oxidation of the Mg/Fe(001) system leads to a different effect [Fig. 6(b)]. O atoms gain 1.59–1.71 electrons from the Mg and Fe atoms. This electron transfer is due to the high electronegativity of the O atoms.

Bader charge differences on the Fe, O, and Mg atoms in Figs. 5 and 6 show direction of the electron flow in each adsorption step, which depends on the adsorption scenario. This is due to the change of the adsorbate atoms position on the surface and significant relaxation of the substrate during the adsorption process. However, for the full MgO monolayer, the absolute values of the Bader charge on the surface Fe, O, and Mg atoms are the same for both adsorption scenarios, and they amount to $7.98e$–$7.99e$, $7.57e$–$7.58e$, and $0.36e$, respectively. For the Fe atoms, the Bader charge increases by about $0.05e$ as compared to the clean Fe(001) surface. A similar increase

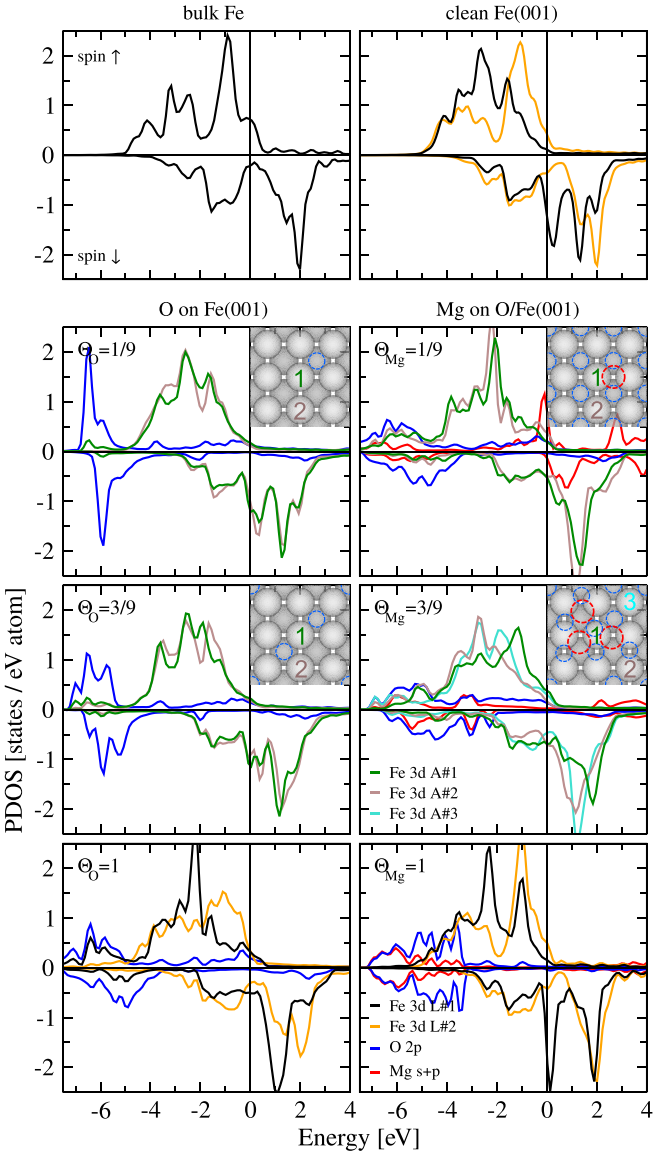

FIG. 7. Partial density of states for different coverages of O and Mg. Zero energy corresponds to the Fermi level. Positive/negative densities correspond to majority/minority states. The plots for Mg states are multiplied by 5. For incomplete coverages, the curves for 3*d* states of Fe atoms are plotted in green, brown, and cyan depending on the atom locations shown in the insets. Blue and red dashed circles in the insets indicate the locations of the O and Mg atoms, respectively, on the surface.

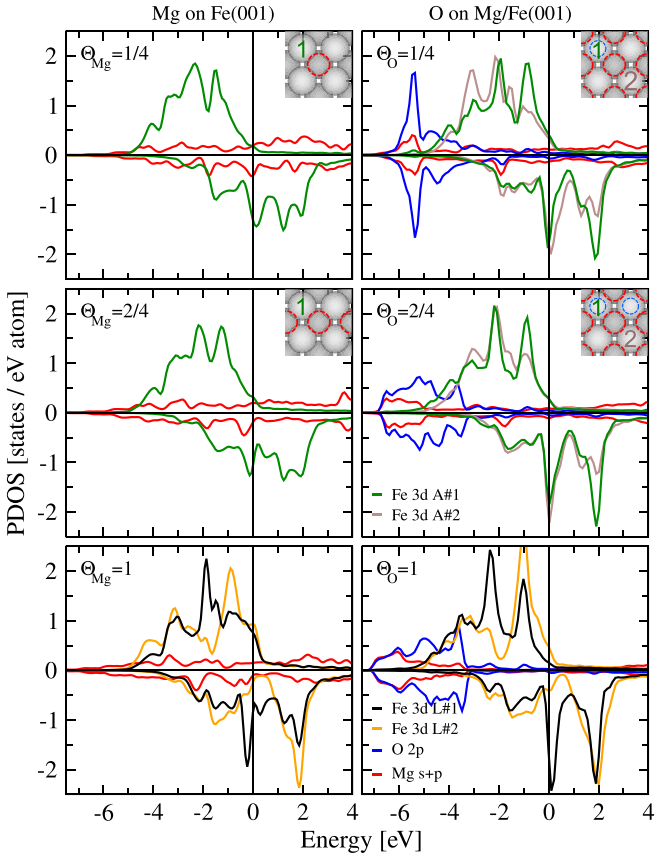

FIG. 8. Same as in Fig. 7 but for different coverages of Mg and O in reverse adsorption scenario.

was observed during the adsorption of the MgO molecules on the Fe(001) surface in our previous work [20].

C. Electronic and magnetic structure

Electronic structure. To investigate the effect of different O and Mg coverages on the electronic structure of the system, we have analyzed changes in the local density of electronic states. Figures 7 and 8 present plots of the partial density of states (PDOS) of the Fe atoms from the first (L#1) and second (L#2) layer, as well as the adsorbate atoms. The densities of 3*d* states of the atoms in the first Fe layer differ, depending on the position of the adsorbate atom. In the first adsorption scenario (Fig. 7), for $\Theta_O = \frac{1}{9}$ and $\frac{3}{9}$, the PDOS of the Fe atoms is only slightly modified in comparison to the states of the clean Fe(001) surface, which suggests a small influence of the oxygen atoms. More significant changes appear for higher O coverage. A strong hybridization between O 2*p* and Fe 3*d* states is observed. This effect is especially pronounced for the majority states below the Fermi level, which results in an enhancement of the magnetic moment. Simultaneously, a significant reduction of the spin polarization at the Fermi level can be noticed. These modifications of the Fe 3*d* states result from a deep immersion of the oxygen in the first Fe layer and its bonding with five Fe atoms, four from the first layer and one from the second layer. The interaction between Fe and O atoms causes strong polarization of the O *p* states. Subsequent adsorption of the Mg atoms in the O/Fe(001) system contributes to further changes in PDOSs. Magnesium binds with O atoms, which causes a shift of the O atoms to other adsorption sites. Consequently, the interaction between oxygen and iron is weakened, which entails a reduction of the magnetic moment. The displacements of the adsorbate atoms on the surface alter the Fe 3*d* states, which strongly depend on local atomic configurations.

Figure 8 illustrates changes in the PDOSs during Mg adsorption on the clean Fe(001) surface and subsequent O adsorption on the Mg/Fe(001) surface. The adsorption of Mg atoms, which provide some electrons to the system, gives rise

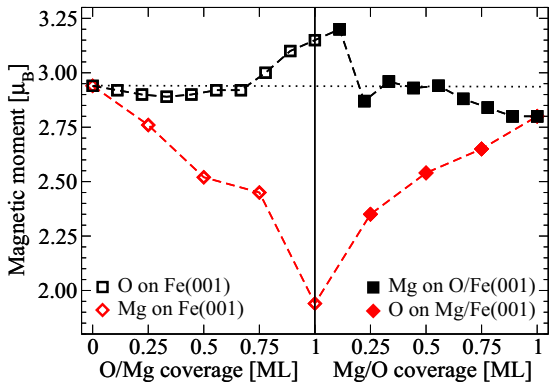

FIG. 9. Average magnetic moment (in Bohr magneton) on the Fe surface atoms versus Mg and O coverage for two different adsorption scenarios. The dotted line indicates the surface magnetic moment value of the clean Fe(001) surface.

to the significant changes in the 3*d* states of the first Fe layer. The presence of magnesium eventually leads to formation of the high minority peak below the Fermi energy and the shift of the majority Fe 3*d* band edge above the Fermi energy. Thus, the magnetic moment in the first Fe layer decreases. In contrast to oxygen, Mg atoms only slightly change the PDOS of the second Fe layer. Subsequent oxidation of the Mg/Fe(001) system leads to the opposite changes. The bonding that appears between O and Mg atoms weakens the Mg-Fe interaction and contributes to a shift of the minority 3*d* states above the Fermi level and enhancement of the magnetic moment on Fe. The shape of the PDOS for $\Theta_O = 1$ is almost the same as in the case of the reverse adsorption scenario.

Magnetic properties. In the first adsorption scenario, for coverages $\Theta_O \leqslant \frac{6}{9}$ ML, the adsorption of O atoms at the hollow sites of Fe(001) only slightly diminishes the average magnetic moment on the surface Fe atoms (Fig. 9). For Θ_O approaching 1 ML, the magnetic moment rapidly increases and reaches $3.15\mu_B$. A relatively high magnetic moment induced on the O atoms ($0.20\mu_B$ for higher Θ_O) is worth mentioning. Such an enhancement of the surface magnetic moments after oxidation is in good agreement with previous theoretical works [28,46]. The adsorption of Mg atoms on the O/Fe(001) surface, initially leads to further increase of the magnetic moment of the surface Fe atoms for $\Theta_{Mg} = \frac{1}{9}$ ML, followed by a substantial drop at $\Theta_{Mg} = \frac{2}{9}$ ML (Fig. 9). Magnetic moments of the Fe atoms depend on the locations of the atoms. Fe atoms located near the Mg atoms have a reduced magnetic moment (2.20–$2.60\mu_B$), whereas the moment values of other Fe atoms are comparable with the values of Fe atoms in the O/Fe(001) system. The average magnetic moment decreases with Mg coverage and achieves $2.80\mu_B$ for the complete MgO monolayer. With increasing Mg coverage, the magnetic moment of the O atoms is reduced to $0.03\mu_B$.

During the adsorption of Mg atoms on the clean Fe(001) surface, the magnetic moment of the Fe atoms strongly decreases with Θ_{Mg}, reaching $1.94\mu_B$ for the full Mg monolayer (Fig. 9), which is less than in bulk Fe ($2.20\mu_B$). This effect shows that nonmagnetic Mg atoms can significantly affect the magnetism of the Fe surface, which is due to additional electrons supplied to the system and contraction of the distance between the first and second Fe layers. A subsequent adsorption of the O atoms weakens the influence of the magnesium on iron and partially restores the surface magnetic moment of iron to $2.80\mu_B$ for the complete oxygen coverage. Similarly, as in the first adsorption scenario, the magnetic moment induced on the O atoms equals $0.03\mu_B$.

IV. SUMMARY AND CONCLUSION

We have investigated the adsorption and coadsorption of the single O and Mg atoms on the Fe(001) surface. The present results confirmed that oxygen adsorption on the clean Fe(001) surface leads to the formation of the stable FeO surface phase with O atoms at the fourfold hollow sites and to enhancement of the surface magnetism [30,31]. On the other hand, the adsorption of magnesium atoms on the clean Fe(001) surface contributes to the considerable reduction of the magnetic moment on the surface Fe atoms.

The adsorption of the Mg atoms on the O-precovered Fe(001) and O atoms on the Mg/Fe(001) surface leads to the formation of the MgO monolayer, with Mg atoms at the hollow sites and oxygen on top of the Fe atoms. In the first case, we found that strong interaction between magnesium and oxygen atoms contributes to a weaker bonding of the O atoms with the iron surface. Consequently, all oxygen atoms are pulled out from the FeO layer. This indicates that even for the oxidized Fe(001) surface, the formation of a sharp MgO/Fe interface is possible. The second adsorption scenario considered, i.e., adsorption of the O atoms on the Mg/Fe(001) substrate, also leads to the formation of a MgO monolayer and confirms experimental findings regarding the formation of a sharp interface between the MgO and Fe layers during oxidation of the Mg-covered Fe(001) surface [22]. The calculated electronic structure and magnetic moments indicate that a full MgO monolayer affects the properties of the Fe surface much weaker than an incomplete MgO adsorbate layer.

Performed calculations show changes in atomic and electronic properties occurring during subsequent stages of the adsorption. Strong interactions and formation of the bonding between adsorbed atoms and the first Fe layer can significantly alter structural, electronic, and magnetic properties of the iron. Our results show complexity of the single steps of the MgO/Fe interface formation, however, the final properties of an ideal MgO/Fe(001) interface do not depend on the growth scenario. On the other hand, any disorder during the growth, leading to deviation from the perfect stoichiometry, can substantially affect the interface type.

The presented results contribute to a better understanding of the MgO/Fe(001) interface structures. The predicted preference of the sharp interface in the ground state under equilibrium conditions shows that diverse and complex interface structures, as observed experimentally, are not system specific and depend on deviation from the ideal structure and on the growth kinetics. Diversification of the atomic structure has a strong impact on the electronic properties. For the sharp MgO/Fe interface, a strong negative spin polarization at the Fermi level is observed as shown also in our previous paper [20] and by Jeon *et al.* [45]. On the other hand, Fe-O bonds in the interface that are formed both for O adsorbed on Fe and on the oxidized MgO/Fe interface, strongly reduce the

spin polarization, which can dramatically modify the transport properties in the Fe/MgO heterostructures [29].

ACKNOWLEDGMENTS

This work was supported by the National Science Center (NCN), Poland (Grant No. UMO-2011/02/A/ST3/00150). We acknowledge provision of computer time from the Interdisciplinary Centre for Mathematical and Computational Modelling (ICM) of Warsaw University (Project No. G44-23). The research was performed in the framework of the Marian Smoluchowski Krakow Research Consortium Leading National Research Centre (KNOW), which is supported by the Polish Ministry of Science and Higher Education.

[1] A. Picone, M. Riva, A. Brambilla, A. Calloni, G. Bussetti, M. Finazzi, F. Ciccacci, and L. Duò, Reactive metal–oxide interfaces: A microscopic view, Surf. Sci. Rep. **71**, 32 (2016).

[2] T. Koyano, Y. Kuroiwa, E. Kita, N. Saegusa, K. Ohshima, and A. Tasaki, The enhanced magnetic moment and structural study of Fe/MgO multilayered films, J. Appl. Phys. **64**, 5763 (1988).

[3] T. Katayama, S. Yuasa, J. P. Velev, M. Y. Zhuravlev, and S. S. Jaswal, Interlayer exchange coupling in Fe/MgO/Fe magnetic tunnel junctions, Appl. Phys. Lett. **89**, 112503 (2006).

[4] J. Faure-Vincent, C. Tiusan, C. Bellouard, E. Popova, M. Hehn, F. Montaigne, A. Schuhl, Interlayer Magnetic Coupling Interactions of Two Ferromagnetic Layers by Spin Polarized Tunneling, Phys. Rev. Lett. **89**, 107206 (2002).

[5] J. Mathon and A. Umerski, Theory of tunneling magnetoresistance of an epitaxial Fe/MgO/Fe(001) junction, Phys. Rev. B **63**, 220403 (2001).

[6] W. H. Butler, X.-G. Zhang, T. C. Schulthess, and J. M. MacLaren, Spin-dependent tunneling conductance of Fe/MgO/Fe sandwiches, Phys. Rev. B **63**, 054416 (2001).

[7] H. X. Yang, M. Chshiev, B. Dieny, J. H. Lee, A. Manchon, and K. H. Shin, First-principles investigation of the very large perpendicular magnetic anisotropy at Fe/MgO and Co/MgO interfaces, Phys. Rev. B **84**, 054401 (2011).

[8] A. Kozioł-Rachwał, W. Skowroński, T. Ślęzak, D. Wilgocka-Ślęzak, J. Przewoźnik, T. Stobiecki, Q. H. Qin, S. van Dijken, and J. Korecki, Room-temperature perpendicular magnetic anisotropy of MgO/Fe/MgO ultrathin films, J. Appl. Phys. **114**, 224307 (2013).

[9] J. F. Lawler, R. Schad, S. Jordan, and H. van Kempen, Structure of epitaxial Fe films on MgO(100), J. Magn. Magn. Mater. **165**, 224 (1997).

[10] A. Subagyo, K. Seuoka, and K. Mukasa, Growth morphology of epitaxial Fe films on annealed MgO(001) surfaces, IEEE Trans. Magn. **35**, 3037 (1999).

[11] J. L. Vassent, M. Dynna, A. Marty, B. Gilles, and G. Patrat, A study of growth and the relaxation of elastic strain in MgO on Fe(001), J. Appl. Phys. **80**, 5727 (1996).

[12] M. Klaua, D. Ullmann, J. Barthel, W. Wulfhekel, J. Kirschner, R. Urban, T. L. Monchesky, A. Enders, J. F. Cochran, and B. Heinrich, Growth, structure, electronic, and magnetic properties of MgO/Fe(001) bilayers and Fe/MgO/Fe(001) trilayers, Phys. Rev. B **64**, 134411 (2001).

[13] T.-Y. Khim, K.-J. Rho, H. Lee, J.-Y. Kim, and J.-H. Park, Investigation for the existence of an iron-oxide layer at the MgO/Fe interface, J. Kor. Phys. Soc. **53**, 1079 (2008).

[14] A. Cattoni, D. Petti, S. Brivio, M. Cantoni, R. Bertacco, and F. Ciccacci, MgO/Fe(001) and MgO/Fe(001)-$p(1 \times 1)O$ interfaces for magnetic tunnel junctions: A comparative study, Phys. Rev. B **80**, 104437 (2009).

[15] H. L. Meyerheim, R. Popescu, J. Kirschner, N. Jedrecy, M. Sauvage-Simkin, B. Heinrich, and R. Pinchaux, Geometrical and Compositional Structure at Metal-Oxide Interfaces: MgO on Fe(001), Phys. Rev. Lett. **87**, 076102 (2001).

[16] H. Oh, S. B. Lee, J. Seo, H. G. Min, and J.-S. Kim, Chemical structure of the interface between MgO films and Fe(001), Appl. Phys. Lett. **82**, 361 (2003).

[17] M. Sicot, S. Andrieu, P. Turban, Y. Fagot-Revurat, H. Cercellier, A. Tagliaferri, C. De Nadai, N. B. Brookes, F. Bertran, and F. Fortuna, Polarization of Fe(001) covered by MgO analyzed by spin-resolved x-ray photoemission spectroscopy, Phys. Rev. B **68**, 184406 (2003).

[18] C. Tusche, H. L. Meyerheim, N. Jedrecy, G. Renaud, and J. Kirschner, Growth sequence and interface formation in the Fe/MgO/Fe(001) tunnel junction analyzed by surface x-ray diffraction, Phys. Rev. B **74**, 195422 (2006).

[19] J. L. Vassent, A. Marty, B. Gilles, and C. Chatillon, Thermodynamic analysis of molecular beam epitaxy of MgO(s) I. MgO vaporization by electron bombardment, J. Cryst. Growth **219**, 434 (2000).

[20] D. Wiśnios, A. Kiejna, and J. Korecki, First-principles study of the adsorption of MgO molecules on a clean Fe(001) surface, Phys. Rev. B **92**, 155425 (2015).

[21] A. Tekiel, S. Fostner, J. Topple, Y. Miyahara, and P. Grütter, Reactive growth of MgO overlayers on Fe(001) surfaces studied by low-energy electron diffraction and atomic force microscopy, Appl. Surf. Sci. **273**, 247 (2013).

[22] O. Dugerjav, H. Kim, J. M. Seo, Growth of a crystalline and ultrathin MgO film on Fe(001), AIP Advances **1**, 032156 (2011).

[23] K. O. Legg, F. Jona, D. W. Jepsen, and P. M. Marcus, Early stages of oxidation of the Fe(001) surface: Atomic structure of the first monolayer, Phys. Rev. B **16**, 5271 (1977).

[24] Y. Sakisaka, T. Miyano, and M. Onchi, Electron-energy-loss-spectroscopy study of oxygen chemisorption and initial oxidation of Fe(100), Phys. Rev. B **30**, 6849 (1984).

[25] J.-P. Lu, M. R. Albert, S. L. Bernasek, and D. J. Dwyer, The adsorption of oxygen on the Fe(100) surface, Surf. Sci. **215**, 348 (1989).

[26] H. Huang and J. Hermanson, Bonding and magnetism of chemisorbed oxygen on Fe(001), Phys. Rev. B **32**, 6312 (1985).

[27] S. R. Chubb and W. E. Pickett, First-Principles Determination of Giant Adsorption-Induced Surface Relaxation in p(1×1)O/Fe(001), Phys. Rev. Lett. **58**, 1248 (1987).

[28] P. Błoński, A. Kiejna, and J. Hafner, Theoretical study of oxygen adsorption at the Fe(110) and (100) surfaces, Surf. Sci. **590**, 88 (2005).

[29] F. Bonell, S. Andrieu, A. M. Bataille, C. Tiusan, and G. Lengaigne, Consequences of interfacial Fe-O bonding and

disorder in epitaxial Fe/MgO/Fe(001) magnetic tunnel junctions, Phys. Rev. B **79**, 224405 (2009).

[30] S. S. Parihar, H. L. Meyerheim, K. Mohseni, S. Ostanin, A. Ernst, N. Jedrecy, R. Felici, and J. Kirschner, Structure of O/Fe(001)-p(1×1) studied by surface x-ray diffraction, Phys. Rev. B **81**, 075428 (2010).

[31] A. Tange, C. L. Gao, B. Y. Yavorsky, I. V. Maznichenko, C. Etz, A. Ernst, W. Hergert, I. Mertig, W. Wulfhekel, and J. Kirschner, Electronic structure and spin polarization of the Fe(001)-p(1 × 1)O surface, Phys. Rev. B **81**, 195410 (2010).

[32] G. Kresse and J. Hafner, *Ab initio* molecular dynamics for liquid metals, Phys. Rev. B **47**, 558 (1993).

[33] G. Kresse and J. Furthmüller, Efficient iterative schemes for *ab initio* total-energy calculations using a plane-wave basis set, Phys. Rev. B **54**, 11169 (1996).

[34] J. P. Perdew, K. Burke, and M. Ernzerhof, Generalized Gradient Approximation Made Simple, Phys. Rev. Lett. **77**, 3865 (1996).

[35] J. P. Perdew, J. A. Chevary, S. H. Vosko, K. A. Jackson, M. R. Pederson, D. J. Singh, and C. Fiolhais, Atoms, molecules, solids, and surfaces: Applications of the generalized gradient approximation for exchange and correlation, Phys. Rev. B **46**, 6671 (1992).

[36] S. H. Vosko, L. Wilk, and M. Nusair, Accurate spin-dependent electron liquid correlation energies for local spin density calculations: a critical analysis, Can. J. Phys. **58**, 1200 (1980).

[37] P. E. Blöchl, Projector augmented-wave method, Phys. Rev. B **50**, 17953 (1994).

[38] H. J. Monkhorst and J. D. Pack, Special points for Brillouin-zone integrations, Phys. Rev. B **13**, 5188 (1976).

[39] M. Methfessel and A. T. Paxton, High-precision sampling for Brillouin-zone integration in metals, Phys. Rev. B **40**, 3616 (1989).

[40] J. Neugebauer and M. Scheffler, Adsorbate-substrate and adsorbate-adsorbate interactions of Na and K adlayers on Al(111), Phys. Rev. B **46**, 16067 (1992).

[41] R. F. W. Bader, *Atoms in Molecules: A Quantum Theory* (Oxford University Press, Oxford, 1990).

[42] G. Henkelman, A. Arnaldsson, and H. Jónsson, A fast and robust algorithm for Bader decomposition of charge density, Comp. Mater. Sci. **36**, 354 (2006).

[43] P. Błoński and A. Kiejna, Structural, electronic, and magnetic properties of bcc iron surfaces, Surf. Sci. **601**, 123 (2007).

[44] T. Shimada, Y. Ishii, and T. Kitamura, *Ab initio* study of magnetism at iron surfaces under epitaxial in-plane strain, Phys. Rev. B **81**, 134420 (2010).

[45] J. Jeon and B. D. Yu, First-principles study of the physical properties of ultrathin MgO films on Fe(001) surfaces, J. Kor. Phys. Soc. **59**, 2291 (2011).

[46] J. Jeon and B. D. Yu, *Ab-initio* study of the interfacial properties in ultrathin MgO films on O-rich FeO/Fe(001) surfaces, J. Kor. Phys. Soc. **65**, 702 (2014).

[47] B. D. Yu and J.-S. Kim, *Ab initio* study of ultrathin MgO films on Fe(001): Influence of interfacial structures, Phys. Rev. B **73**, 125408 (2006).

[48] A. Kiejna, Work function of metals, in *Reference Module in Chemistry, Molecular Sciences and Chemical Engineering*, edited by J. Reedijk (Elsevier, Waltham, MA, 2014), pp. 1–8.

[49] E. Wachowicz and A. Kiejna, Bulk and surface properties of hexagonal-close-packed Be and Mg, J. Phys.: Condens. Matter **13**, 10767 (2001).